Received: 5 August 2023 | Revised: 7 January 2024 | Accepted: 8 January 2024

DOI: 10.1111/gcb.17172

Global Change Biology WILEY

RESEARCH ARTICLE

Increased belowground tree carbon allocation in a mature mixed forest in a dry versus a wet year

Ido Rog[1] | Boaz Hilman[2,3] | Hagar Fox[1] | David Yalin[4] | Rafat Qubaja[4] | Tamir Klein[1]

[1]Department of Plant & Environmental Sciences, Weizmann Institute of Science, Rehovot, Israel

[2]Department of Biogeochemical Processes, Max-Planck Institute for Biogeochemistry, Jena, Germany

[3]The Institute of Earth Sciences, The Hebrew University of Jerusalem, Jerusalem, Israel

[4]Department of Earth and Planetary Sciences, Weizmann Institute of Science, Rehovot, Israel

Correspondence
Ido Rog and Tamir Klein, Department of Plant & Environmental Sciences, Weizmann Institute of Science, Rehovot 76100, Israel.
Email: ido.rog@weizamnn.ac.il and tamir.klein@weizmann.ac.il

Present address
Ido Rog, Plant–Soil Interactions Group, Research Division Agroecology and Environment, Agroscope, Zurich, Switzerland

Rafat Qubaja, School of Sustainability, Arizona State University, Tempe, Arizona, USA

Funding information
Jewish National Fund (KKL) Forest Department; Sustainability and Energy Research Initiative; European Research Council, Grant/Award Number: RHIZOCARBON

Abstract

Tree species differ in their carbon (C) allocation strategies during environmental change. Disentangling species-specific strategies and contribution to the C balance of mixed forests requires observations at the individual tree level. We measured a complete set of C pools and fluxes at the tree level in five tree species, conifers and broadleaves, co-existing in a mature evergreen mixed Mediterranean forest. Our study period included a drought year followed by an above-average wet year, offering an opportunity to test the effect of water availability on tree C allocation. We found that in comparison to the wet year, C uptake was lower in the dry year, C use was the same, and allocation to belowground sinks was higher. Among the five major C sinks, respiration was the largest (ca. 60%), while root exudation (ca. 10%) and reproduction (ca. 2%) were those that increased the most in the dry year. Most trees relied on stored starch for maintaining a stable soluble sugars balance, but no significant differences were detected in aboveground storage between dry and wet years. The detailed tree-level analysis of nonstructural carbohydrates and $\delta^{13}C$ dynamics suggest interspecific differences in C allocation among fluxes and tissues, specifically in response to the varying water availability. Overall, our findings shed light on mixed forest physiological responses to drought, an increasing phenomenon under the ongoing climate change.

KEYWORDS
belowground, carbon allocation, carbon balance, drought, lipids, mixed forest, nonstructural carbohydrate

1 | INTRODUCTION

Intensification of drought frequency driven by climate change leads to a strong reduction in the amount of carbon (C) trees sequester (Chiang et al., 2021; Joos et al., 2001). Drought-stressed plants may also reach their physiological thresholds, leading to ecosystem decline (Berdugo et al., 2022). Exceptional resilience to drought was found in mixed forests, which host various tree species with different C allocation strategies (Rog, Tague, et al., 2021; Schnabel et al., 2021; Werner et al., 2021). However, the forest-scale methods like eddy covariance and canopy imaging might be insufficient, requiring species-level measurements of all C pools and fluxes (Baldocchi et al., 2001; Richardson, 2019). Such tree-level measurements can reveal species-specific mechanisms involving C allocation between

tree compartments (Klein & Hoch, 2015), C storage build-up and use, and relations to water use (Babst et al., 2014; Mund et al., 2010). To date, C allocation studies at the tree level are rare in water-limited environments such as semi-arid and Mediterranean mixed forests. These systems are instrumental as they represent a significant part of the globe and can contribute to the understanding of forest dynamics in a future drier climate.

In both global C cycle simulations and direct measurements, the C budgets of terrestrial plants are rarely balanced (Le Quéré et al., 2016; Marshall et al., 2023), indicating missing C sinks. The missing sinks are probably belowground fluxes that are difficult to measure, like root growth and C transfer to the rhizosphere (Crowther et al., 2019; Klein, Bader, et al., 2016; Schiestl-Aalto et al., 2019). In local observations and global estimates alike, trees allocate more C belowground in water-limited environments (Brunn et al., 2023). Globally, the region with the highest proportion of roots in total biomass is the Mediterranean region (Ma et al., 2021). Trees growing in more arid climates also have shorter shoots but deeper and narrower root systems (Tumber-Dávila et al., 2022). In addition, trees exposed to drought reduce the rooting zone area (Gao et al., 2021); exudate more C into the soil (Brunn et al., 2022, 2023); and probably grow roots to deeper soil layers.

The challenge in studying the relationships between photosynthesis, C transport, and belowground C is to follow the different fluxes simultaneously over extended time scales, that is, months and years. However, to study the in situ response to climatic change, there is a need for multi-annual research. To address this challenge, $^{13}CO_2$ labeling may be advantageous (Epron et al., 2012; Sala et al., 2012), but in mature forests, and specifically in mixed forests, this would require massive investment. Thus, the more traditional C mass balance approach is the only viable way to attain a comprehensive quantification of C fluxes (Ågren et al., 1980). For this approach, whole-tree C fluxes and pool size changes are determined with time resolutions between months and seasons. The method allows quantifying the rate of C transfer among compartments, the residence time in each compartment, and the specific metabolic compound being stored in the compartment (Klein & Hoch, 2015). Previous work has shown that the mass balance approach is able to distinguish between C allocation dynamics in different tree species with different seasonal behaviors (Le Roux et al., 2001; Rog, Jakoby, & Klein, 2021) and in response to abiotic factors like elevated CO_2 (Dror & Klein, 2022; Wegener et al., 2015).

The ability to store and use nonstructural carbohydrates (NSC) and lipids is thought to contribute to tree survival. The stored C can provide energy and C skeletons when newly fixed carbon amounts are too low, as during drought when stomatal conductance is reduced. Hence, the dynamics of storage compounds like NSC were suggested to indicate tree resilience to drought (Hoch & Körner, 2012; O'Brien et al., 2014; Signori-Müller et al., 2021). NSC levels drop when the balance between demand and supply is skewed, while resilient trees continue to grow, as growth is permitted by sufficient turgor (Zweifel et al., 2021). NSC reduction during drought is expected to be smaller than in vulnerable trees, by minimizing activities of C sinks like growth. In saplings, NSC decreases after severe drought years, especially in the root (He et al., 2020); however, in mature trees, no NSC decrease was detected (Hesse et al., 2021). In addition to drought, C supply affects NSC levels and can be reduced under long C-limitation in trees. Shade-tolerant tree species maintain high NSC levels as a strategy to recover faster from disturbance (Poorter & Kitajima, 2007). On the other hand, tree species with light-demanding characteristics allocate more C to growth and invest less in NSC storage (Poorter & Kitajima, 2007). However, in water limited but not light-limited environments, the link between NSC storage and light requirements is weaker (Poorter & Kitajima, 2007). Understanding the annual and seasonal NSC storage dynamics can help define the resilience strategy of each tree species.

Our goal in this study was to provide the first comprehensive tree-scale carbon allocation dynamics in a mixed Mediterranean forest and its response to climatic conditions. We assessed the monthly mass balance of C assimilation and investment in above- and belowground C sinks in 20 mature trees of five species growing together in a forest stand. The 2 years of the study period covered not only the seasonal dry period but also two contrasting hydrological years, one with 25% lower rainfall and the following with 21% higher rainfall than average (Figure 1). To evaluate the resilience of the trees, we measured storage pools NSC and $\delta^{13}C$ on a seasonal basis. In non-water-limited environments and less resilient tree species, drought can strongly reduce sink activity and thus C allocation belowground (Joseph et al., 2020; Ruehr et al., 2009; Zwetsloot & Bauerle, 2021). However, in water-limited environments, drought-induced shifts in C allocation are mainly belowground, but the exact mechanism is poorly known. In our water-limited environment, we hypothesized that trees would invest more C belowground in the dry periods, assuming water is the limiting factor and can be taken up by investing in root development belowground. Furthermore, precipitation will affect the C allocation dynamic mainly by reducing assimilation and total sinks in the dry year. Finally, we expect a larger NSC reduction during water stress periods and less negative $\delta^{13}C$ values in drought-resistant trees.

2 | MATERIALS AND METHODS

2.1 | Site and study design

Field measurements of mature trees were conducted in a 1 ha forest research plot at the Judean foothills in Israel (Yishi forest, 31° 43′ N, 34° 57′ E, 320 m elevation; Klein et al., 2013; Lapidot et al., 2019; Rog, Tague, et al., 2021). The climate is Mediterranean, with annual precipitation of 510 mm falling between September and May, rendering May–September as a prolonged drought. The mean diurnal temperatures are 16.0°C in February and 25.3°C in August. The vegetation is dominated by the conifers *Pinus halepensis* and *Cupressus sempervirens*, planted ca. 50 years ago. Shortly after the planting, the local broadleaf woody species *Quercus calliprinos*, *Ceratonia siliqua*, and *Pistacia lentiscus* started to resprout in the stand. Since forest management was minimal, we assume natural tree growth.

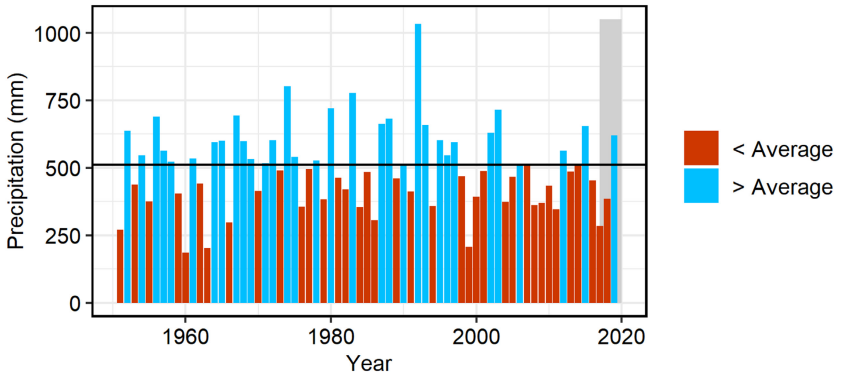

FIGURE 1 Variability in precipitation amounts in the study mixed Mediterranean forest. Dry years, yearly precipitation below average ($P_{average}$ = 511 mm), and wet years are above average. Carbon allocation measurements in this study were from representative dry year (P_{2018} = 384 mm, dry), and high precipitation year (P_{2019} = 621 mm, wet) marked by a gray background. Note that preceding years were also dry: P_{2016} = 454 and P_{2017} = 285. Precipitation data are from Beit Jimal meteorological station (1 km east of the study stand).

The forest canopy is dominated by the relatively tall conifers, especially the *Pinus*, with lower-stature *Quercus*, *Ceratonia*, and *Pistacia*. Considering >1 m height individuals, we monitored by GPS instrument (eTrex30x; Garmin, Olathe, USA) 242 *Pistacia*, 146 *Cupressus*, 109 *Quercus*, 31 *Pinus*, and 9 *Ceratonia* trees. Stand density, accounting only for ca. 50-year-old individual is 134 trees ha^{-1}. For more information about forest density and tree distribution, see Rog, Tague, et al. (2021). We selected 4–10 mature trees of each of the five studied species.

2.2 | C mass balance of mature trees

During two consecutive hydrological years (October 2017–September 2019), we assessed monthly C mass pool sizes and fluxes and upscaled them to the compartment and tree levels. For this purpose, we combined direct and indirect measurements and data from previous onsite studies (Table S1, Figure S1). While we obtained data about the tree compartments: stem (including bark), branches and twigs, reproductive tissues, foliage, root collar, coarse roots, and fine roots (Tables S2, S3). For further analyses, we aggregated the data into the four compartments: wood, reproductive tissues, foliage, and roots (detailed in Table S1). Allometric equations for the different tree species were used for creating compartment-specific total area (Table S2) and the C mass pool dataset (Table S3; Rog, Tague, et al., 2021). We additionally evaluated the content of the non-structural carbohydrates (NSC) starch and soluble sugars in woody branches. We focused on this tissue because woody tissues contain the largest absolute storage pools in trees (Furze et al., 2019; Hoch et al., 2003), and because extracting stem cores multiple times can be fatal for the trees. Carbon fluxes were based on in situ measurements conducted for more than 3 years (2017–2020; Table S1). We measured six fluxes: photosynthetic assimilation, reproduction, respiration, growth, litter, and exudation (to focus on the tree-scale C allocation, the term "flux" is also used for growth, litter, and reproduction). The frequency of the measurements ranged from once every 2 weeks to once a year (Table S1). To integrate all measurements, we transformed the results into means of diurnal flux rates ($g\,C\,tree^{-1}\,day^{-1}$). The mean and standard error for all fluxes are calculated among the four individual trees of the five tree species. For the annual scale, the sum of the representative day of the month was multiplied by the number of days (averaged month value calculated for bi-monthly measurements). A further explanation of the specific measurement and calculation for the six fluxes is presented below.

2.3 | Carbon assimilation flux

Net C assimilation was measured using two methods: leaf scale and tree-level scale. Leaf-scale measurements were measured bi-monthly (approximately every 2 weeks) using an infrared gas analyzer (IRGA) with a portable gas exchange and fluorescence system (averaged of morning, noon, and after noon measurements, GFS-3000, WALZ, Effeltrich, Germany, Rog, Tague, et al. (2021)). The five tree species varied in height and canopy structure (Table S2), thus all leaf-scale measurements were from sun-exposed leaves at the same height (1–2 m) except for *Pinus* trees (6–8 m) with three-fold higher canopies compared to the other tree species. We used allometric equations for upscaling to the tree-scale net assimilation flux (A_{tree}) and multiplied by the light hours per day in every month (assuming the two measurements per month capturing the monthly variability). In a complementary method used to verify the leaf-scale measurements, A_{tree} was calculated using sap flow measurements available for four species (Klein, Rotenberg, et al., 2016; Rog, Tague, et al., 2021; *Pistacia* trees were not measured because of the small stem diameter). All the equations and calculations of converting sap flow measurements into tree assimilation are described in (Klein, Rotenberg, et al., 2016). The conversion is based on the physiological relationship between instantaneous water use efficiency (WUEi) multiplied by g_s to calculate A_{tree}. In order to estimate g_s, we calculated T_{tree} from sap flow divided by VPD values taken from the meteorological station (described in section

"*Environmental conditions and their monitoring*", online dataset). WUEi calculated based on $\delta^{13}C$ values (described in section "*$\delta^{13}C$ analysis*," online dataset). Sap flow measurements are described in Rog, Tague, et al. (2021). Briefly, sap flux density measurements were taken approximately every 2 months using heat balance sensors (EMS, Brno, Czech Republic). To avoid installation artifacts, metal slots were continuously installed on tree stems, and probes were added only during measurement campaigns. Sensors measured for 2–4 days, logged every 10 min, and calculated sap flow for the sapwood area (ignoring the bark). WUEi was calculated based on the significant relationship between stomatal regulation, WUEi, and $\delta^{13}C$. Here we used young branches (1–2 years) and not leaves, which are more affected by diurnal changes. The year 2019 is a good proxy for $\delta^{13}C$ accumulation of the dry year because it came in a third below-average year, and the high assimilation flux in 2020 introduced a relatively high C amount to the branch C pool (description of $\delta^{13}C$ measurements are in "*$\delta^{13}C$ analysis*" section). A linear relation was found between the two assimilation measurement methods, measured on the exact same days (Figure S2), with mildly lower leaf-scale estimation (vs. whole-tree measurement) and higher leaf-scale estimation for conifers and broadleaves, respectively. The assimilation values calculated at the leaf scale were corrected according to the linear relation between the two measurement methods. Thus, we were able to use the relatively frequent leaf-scale measurements (every 2 weeks) corrected with the tree-scale measurements. Using these two independent approaches, based on different physiological concepts, provided more accurate net assimilation values.

2.4 | Respiration flux

To estimate respiration rates, we measured CO_2 efflux from leaves, stems, and roots (Table S2). Dark foliage respiration (mitochondrial dark respiration) was measured monthly, after the sun set, using IRGA leaf gas exchange with four replicates per species (Rog, Tague, et al., 2021). We assumed dark respiration can be measured during the day by darkening the leaf at a given temperature and month (Farquhar & Busch, 2017; Tcherkez et al., 2009). IRGA settings parameters were similar to the assimilation measurements, with top and bottom covers for light access (Rog, Tague, et al., 2021), and upscaled to the corrected tree scale. We measured stem CO_2 efflux in bi-monthly intervals over 1 year (January 2017–April 2018) using a static stem chamber (Hilman & Angert, 2016). After incubation of 1 h, we sampled the chamber headspace in a flask and measured the CO_2 concentration using an IRGA (LI 840A, LI-COR, Lincoln, NE, USA). Measuring root respiration in situ is challenging because it requires airtight incubation of intact roots, which is difficult to achieve. We alternatively estimated the root respiration fraction from total soil respiration (Rs), which we estimated by measurements and previous data. Root respiration fraction from Rs was measured with incubations of excised roots from the ingrowth cores (more details in the *growth* flux section) during January 2019. In this campaign, ingrowth cores were extracted and inserted directly into the IRGA 3010-A chamber. Rapidly, after stable measurement of the entire ingrowth core contents, fine roots were sieved and only fine roots were inserted for a second measurement. This experiment provides information about the fraction of root respiration from Rs (Figure S3) and about fine-root respiration in 0.2 m depth soil, which we extrapolated with fine-root biomass for another estimation of total root respiration. Root respiration fractions were approximately 0.25–0.35 for soil samples below the five tree species. Based on (Qubaja, Tatarinov, et al., 2020), we assume small differences in the root respiration fraction from the entire soil respiration among seasons. Thus, the monthly dynamic of root respiration from Klein and Hoch (2015) was multiplied with the total amount of root growth per individual tree to get the most accurate estimation of root respiration in the site. Knowing the limitations of this root respiration approach, we confirmed the fraction of root respiration from total soil respiration approaches. By estimating the fraction of root respiration from total soil respiration (Table S4). Soil respiration was measured in a nearby plot (less than 1 km from the intensively measured plot and with identical characteristics) on non-disturbed soil during the dry (Sep) and wet (Nov) seasons. The soil CO_2 flux (Rs) was measured with an automated non-steady-state system (LI-8100A; LI-COR, Lincoln, NE, USA), using opaque chambers 20 cm in diameter (Long-Term Chambers; LI-8100-104; LI-COR) and a multiplexer (Multiplexer; LI-8150; LI-COR) to allow for the simultaneous control of several chambers (described in detail in (Qubaja, Tatarinov, et al., 2020)). The chamber was closed on preinstalled PVC collars (20 cm in diameter, inserted 5 cm into the soil, and 6 cm above the surface) for 2 min and was positioned away from the collar the rest of the time. The air from the chambers was circulated at 2.5 L min^{-1} through the IRGA and were logged in the system logger (1 s^{-1}) half hourly.

2.5 | Carbon allocation to growth

Carbon allocation to growth was measured and calculated separately for each of the three compartments: foliage, stem, and roots. Foliage growth was measured and verified with three methods: Annual dynamics were measured by needle length increment in *Pinus* and by photos and area increment calculation for the other species (using ImageJ; (Rueden et al., 2017)). For the latter, we used three technical replications per tree. Values calculated from images were in low quality in part of the data points, and values from *Pinus* needle growth were complemented where needed by assuming the similar growth rate. A complementary method was included the leaf longevity of each tree species (downloaded from the TRY database (Kattge et al., 2020)) for the estimation of annual leaf growth. Mean monthly foliage growth was calculated by the total mean growth per year divided by the measured proportion of the growth every month, reflecting the species-specific flush growth behavior among the species. Finally, the calculated

annual foliage growth was verified using the annual foliage litter production (measured directly; see *litter* flux methods). Annual stem growth was calculated by the mean annual DBH increment, which was measured bi-monthly using band dendrometers (UMS, D1, Alton, England) installed on 10 trees from each species since October 2016. Species such as *Quercus* and *Ceratonia* trees with multistems (3–4 stems) were measured in only one stem and were assumed to grow at similar rates in all the stems. Multistems *Pistacia* trees were too small for the band dendrometers; thus, manual stem growth diameter was measured using a caliper. With no growth during the end of the dry season, the baseline growth of every year was set to September stem size. Root growth was measured using the ingrowth core method, assuming root growth is mostly in the top soil and dominated by fine-root growth (Dror & Klein, 2022; King et al., 2002). Twelve ingrowth cores (length: 0.12 m, diameter: 0.03 m, mesh size: 3 mm) were installed in 1-m distance from the main stem of every tree ($n = 4$) in groups of three, covering the entire tree area (Figure S4). Every group of three cores was averaged, and the four groups were used as technical replications to calculate the annual root growth $year^{-1}$ $area^{-1}$ below every tree. The root growth monthly dynamic was taken from Klein and Hoch (2015). We adjusted the monthly dynamics by minirhizotron data from a pine forest site located 50 km south from our site. Tubes were buried in the soil at ca. 30 cm depth and 1 m from the tree's stem. We used the portable imager CI-600 In-Situ Root Imager (CID Bio-Science, Camas, WA, USA) and the RhizoTrak plugin at ImageJ software to analyze the images. Once a month, a panoramic image from every tube was captured and compared to previous imaging sessions. Over the time-series images, the length for each individual root was calculated and divided by the number of days since the last imaging session to produce the specific growth rate. We assumed a similar dynamic for the different tree species, but species-specific amounts according to ingrowth core data.

2.6 | Litter production and reproduction

The production of aboveground litter and reproduction tissues were quantified using litter traps installed below the canopy of each tree species ($n = 4$). Three litter traps (0.5×0.2 m) were installed below every tree (used as technical replications), from which litter was collected bi-monthly. The oven-dried samples (60°C, 48 h) were identified for tree species, separated manually into leaf, branch (woody tissues), and reproduction tissues, and weighted with an analytical balance (Mettler Toledo, Columbus, Ohio, UAS). The production of the three litter tissues were upscaled to a single tree basis by multiplying the ratio between the tree crown area of every tree and the litter trap area. Root litter was estimated using the global patterns of root turnover in the terrestrial ecosystem database (Gill & Jackson, 2000), assuming each conifer and broadleaf group share the same root turnover rate.

2.7 | Root exudation flux

Root-exudation data for the *Cupressus* and *Pistacia* in our site were previously published (Jakoby et al., 2020). The exudation rates measured during 2017 and 2018 were negatively correlated with leaf assimilation rate (Jakoby et al., 2020). We used our assimilation rates and the correlation coefficients to calculate exudation rates in 2019. Assuming no large differences among species in the two functional groups (conifers and broadleaves; Dror & Klein, 2022; Rog, Tague, et al., 2021), we extrapolated the exudation rates to the unmeasured species. In addition, the rate of exudate C was assumed to be in proportion to the amount of C allocated to fine-root annual growth and the total fine-root compartment mass (Table S3).

2.8 | Branch NSC

Nonstructural carbohydrates (NSC) were measured in non-photosynthetic branches that were collected every 3 months (approximately every season). Immediately after sampling, we terminated metabolism by a heat shock (3 cycles of 2-min microwave). Samples were then oven-dried for 48 h and powdered using a grinder. We then prepared 30 ± 0.1 mg aliquots for NSC analysis (Landhäusser et al., 2018; Tsamir-Rimon et al., 2021). Soluble sugars were extracted using 80% ethanol. We then converted the starch in the pellet to glucose using the enzymes alpha-amylase (cat no. G3293-50ML; Sigma Aldrich, St Louis, MO, USA) and amyloglucosidases (LYO., SQ (500 U)). The sugars glucose, fructose, and sucrose were separated in an ultra-high-speed liquid chromatography (UFLC) system (Shimadzu Scientific Instruments, Kyoto, Japan) fitted with an Aminex HPX-87C Column (300×7.8 mm, 9 µm particle, Bio-Rad, California, USA) and refractive-index detector. Conditions of sugars separation were set according to manufacturer recommendations (84°C column temperature, water as mobile phase, 0.6 mL/min flow rate). Soluble sugars and degraded starch samples were run separately and quantified using standard curves of known concentration (Sigma cat. 47,829, 47,289, and F2793). Internal standard (pure glucose, starch standard, and HPLC standard) were used to monitor the quality of the analysis routinely between samples. NSC content was calculated as glucose equivalent on a % dry matter basis.

2.9 | Stem lipids and NSC analysis

Lipids were extracted from tree stem samples using a modified Bligh and Dyer (1959) protocol. Our extraction is not quantitative because we replaced the efficient but toxic original solvent chloroform with dichloromethane (DCM). Yet, the results allow between-species comparison. The measured samples were composites of two cores taken from the northern and eastern aspects of the stems in December 2020. We milled the sapwood from the outer 2 cm and prepared 100-mg aliquots. The aliquots were first sonicated for 15 min in

methanol and DCM solution (7.5 mL:4 mL). Then we discarded water-soluble compounds by repeating three times the following: addition of water:DCM (4 mL: 4 mL) solution, centrifuge at 733 ***g*** for 10 min, and removal of the upper water phase. Then the lower phase was water-dried over sodium sulfate, reduced to the same volume, and quantified gravimetrically. Stem NSC were measured according to the Landhäusser et al. (2018) protocol describe in the branch NSC method section. To test if NSC stocks can fuel the C fluxes during the drought year and balance the C budget, we measured species-specific "Maximum annual NSC" in branches and main stems, and obtained NSC data for foliage and roots from published studies (Table S10). The highest annual concentration of each compartment (foliage, branch, stem, and root) in percentage (weight/weight) was multiplied by the compartment mass (kg C per year, Table S10). Stem NSC assumed to low annual variation (Smith et al., 2018) and was hence measured once, in December 2020, using stem cores.

2.10 | δ ^{13}C analysis

Non-photosynthetic young branches were collected once every season (the same samples as the NSC analysis), oven-dried at 60°C for 48 h, and kept dry until grinding. An amount of 1 mg of dry tissue biomass was weighed in a tin capsule and installed onto a combustion module equipped with an auto-sampler (ECS 4010, Costech Analytical, Valencia, CA, USA). The resultant CO_2 gas product was analyzed with the ^{13}C analyzer, ^{13}C cavity ring down spectroscopy (CRDS; Picarro G2131i, Picarro, Santa Clara, CA, USA; <0.1‰ precision, <0.5‰ drift for δ^{13}C in CO_2), which was directly interfaced to the combustion module. Results were expressed as parts per thousand (‰) deviations from the international C isotope standard (Vienna Pee Dee Belemnite, VPDB). An international standard (IAEA-CH-3 (−24.724‰), Cellulose, International Atomic Energy Agency, Vienna, Austria; Verkouteren, 2006) was used, and internal standards (glucose, 11.1‰) were used for every nine samples.

2.11 | Environmental conditions and their monitoring

The meteorological information was provided by the Israel Meteorological Service (IMS) station at Beit Jimal, located 1 km east of our measured forest plot and at the same elevation. Maximum air temperature and maximum relative humidity were measured at a standard height of 2 m aboveground. Maximum air temperature and maximum air humidity data were further used to calculate the vapor pressure deficit (VPD), as outlined in Lapidot et al. (2019). We measured soil water content (%, v/v) in the site using a dielectric constant EC-5 soil moisture sensor connected to an Em50 data logger (Decagon Devices Inc., Pullman, WA, USA), which was programed to record observations at 30-min intervals. The sensors were located in two places in the center of the measured forest plot, at soil depths of 5 and 25 cm. Solar radiation data (global radiation, W/m^2) were downloaded from the Beit Dagan IMS station located 45 km from the measured plot (Figure S5).

2.12 | Upscaling from tree to forest scale

The annual species-specific C fluxes were upscaled to the forest level using the relative stand densities of each of the five tree species (mentioned in the *Site and study design* section and in Rog, Tague, et al., 2021) to g C m^{-2} year^{-1} units. The flux means and standard errors were calculated for the four replicas of each tree species multiplied by its stand density to obtain four putative forests with the same relative stand density. In addition, for every flux, the relative percentage from the entire forest C flux was calculated.

2.13 | Statistics

Data were calculated and visualized using R (Team, 2000) and the interface R Studio (Team, 2018). We evaluated the effects of several environmental factors and soil water content on tree species and C flux (g C tree^{-1} day^{-1}) using a set of general linear mixed models (GLMM's). We used the user interface Jamovi (The Jamovi project, 2021) and particularly the package "gamlj" (Gallucci, 2024) for GLMM. A nested design was used to generate random factors (individual trees of each species and the month of measurement) and calculate the variance partitioning of the C allocation across different fluxes, species, and whether they originated from above/belowground (all model formulas are presented in Tables S5–S8; statistical commands are available in the tables). In all models, the fluxes, species, and above/belowground were considered as a fixed factors, while the individual trees of each species and the month measurement were considered as nested random effect. We included the precipitation, maximum air temperature, minimum air temperature, maximum VPD, solar radiation, and soil water content in 5 and 25 cm as covariates in the models.

3 | RESULTS

3.1 | Carbon allocation patterns

The C source (photosynthesis) and sum of C sinks (reproduction, respiration, growth, litter, and exudation) per year were nearly balanced, with fluxes of 70–90 kg C tree^{-1} year^{-1} in conifers, 60 kg C tree^{-1} year^{-1} in *Ceratonia*, and less than 20 kg C tree^{-1} year^{-1} in *Quercus* and *Pistacia* (Figure 2a). The observation of nearly balanced fluxes strengthens our confidence in the method. The source flux was significantly higher than the sink flux in the wet year across the tree species except for *Pistacia* (*species* × *flux* × *year*, $F_{32,89} = 3.030$, $p < .001$; Figure 2a, Table S5). During the dry year, the source flux declined while the sink flux maintained its magnitude, resulting in a negative C balance of 3–20 Kg C tree^{-1} year^{-1}. Carbon partitioning

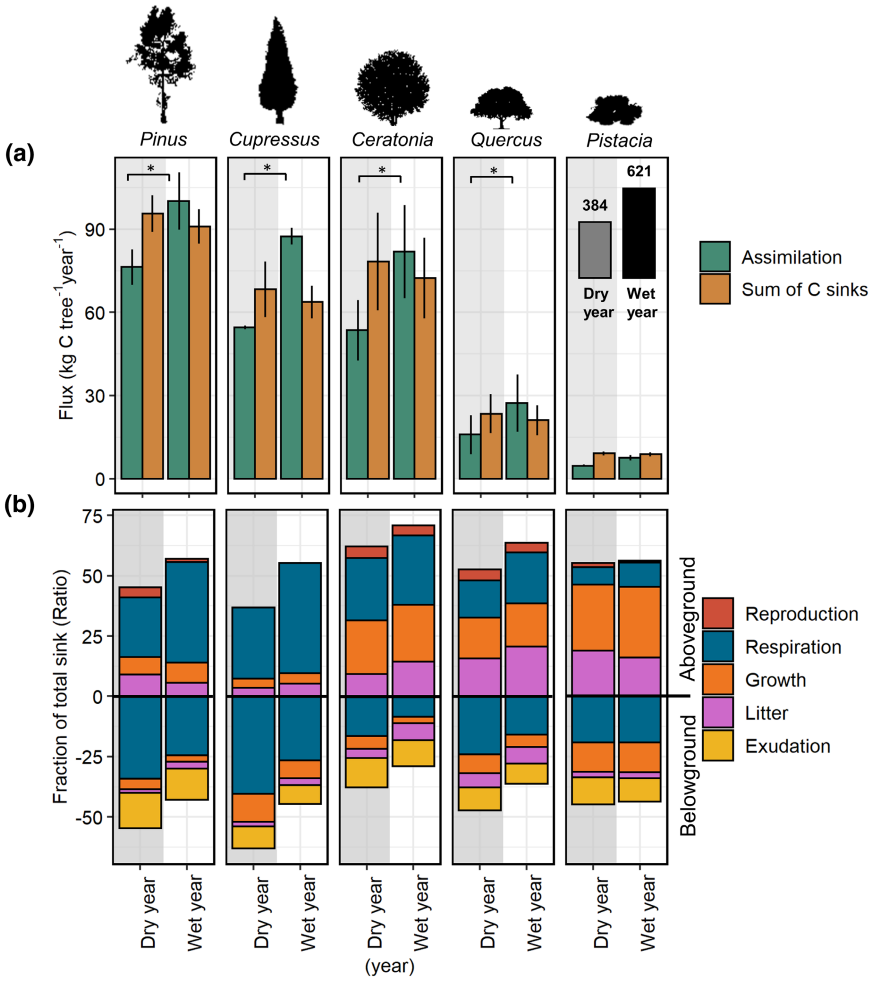

FIGURE 2 Carbon balance and carbon partitioning aboveground and belowground in dry and wet years in five species of the mixed Mediterranean forest. (a) Carbon (C) source (assimilation) and sum of the five main C sinks in kg C $tree^{-1} year^{-1}$. Asterisks are for significant differences (species × year × flux, $p < .001$, $n = 4$). (b) Carbon partitioning to the five main C sinks: reproduction, respiration, growth, litter, and exudation dividing to aboveground and belowground allocations. Ratio values assuming C balance between sources and sinks. The gray background represents the dry year.

among the five main C sinks was significantly different among species (*species* × *flux*, $F_{32,89} = 59.107$, $p < .001$; Figure 2b). Respiration was the main C sink in all species except *Pistacia*, which invested most of its C in growth. Dividing the sinks to aboveground versus belowground revealed larger belowground sinks (mainly respiration) during the dry year in all species, with the strongest effect in *Pinus*, *Cupressus*, and *Quercus* (*species* × *year* × *above*, $F_{4,89} = 2.519$, $p < .039$; Figure 2b).

3.2 | Seasonal and annual imbalances between source and sink

Assimilation flux in trees, except *Ceratonia*, showed a bell-shaped seasonal pattern with the highest flux during February–April (Figure 3). An additional and later peak was observed in some species in the wet year (Figure 3). Daily assimilation ranged from >500 g C $tree^{-1} day^{-1}$ for the *Pinus* and *Cupressus* trees, while *Ceratonia*, *Quercus*, and *Pistacia* trees assimilated 300, 100, and 50 g C $tree^{-1} day^{-1}$, respectively. The peak of the total C sinks lagged 1–2 months behind the source peak and came earlier in the dry year compared to the wet year (Figure 3). The total sinks consumed less or equal amount of C than assimilated, except for April–July (Figure S6). The peaks of the individual fluxes followed each other: respiration in winter, growth in spring, litter production in late spring, and root exudation in summer. During the dry year, species-specific responses of increased reproduction in the *Pinus* and elevated respiration for the *Cupressus* were observed.

3.3 | C storage dynamic in dry and wet years

Concentrations of starch (0%–15% of dry weight, DW) and sugars (1–5% DW) varied among species, years, and seasons (GLMM, details in Table S6; Figure 4). Overall, starch content showed greater inter-seasonal and inter-annual variability compared to soluble sugars. Starch dynamics followed the assimilation bell-shape dynamic in the two conifers with a winter–spring maximum of 6%–10% and a summer–autumn minimum (*year* × *species*, $F_{12,39} = 2.33$, $p = .058$). Significant differences between dry year and wet year were detected in *Quercus* starch and in *Ceratonia* soluble sugars (*year* × *species*; $F_{4,39} = 3.33$, $p = .005$; $F_{4,39} = 2.55$, $p = .023$, Table S7). The seasonal effect for Quercus was weaker (*Quercus*, *year* × *species*, $F_{12,39} = 3.51$, $p > .14$). In *Pistacia*, starch was detected only in the autumn, winter, and the dry year's spring. The concentrations of the soluble sugars were significantly different along the seasons and the years

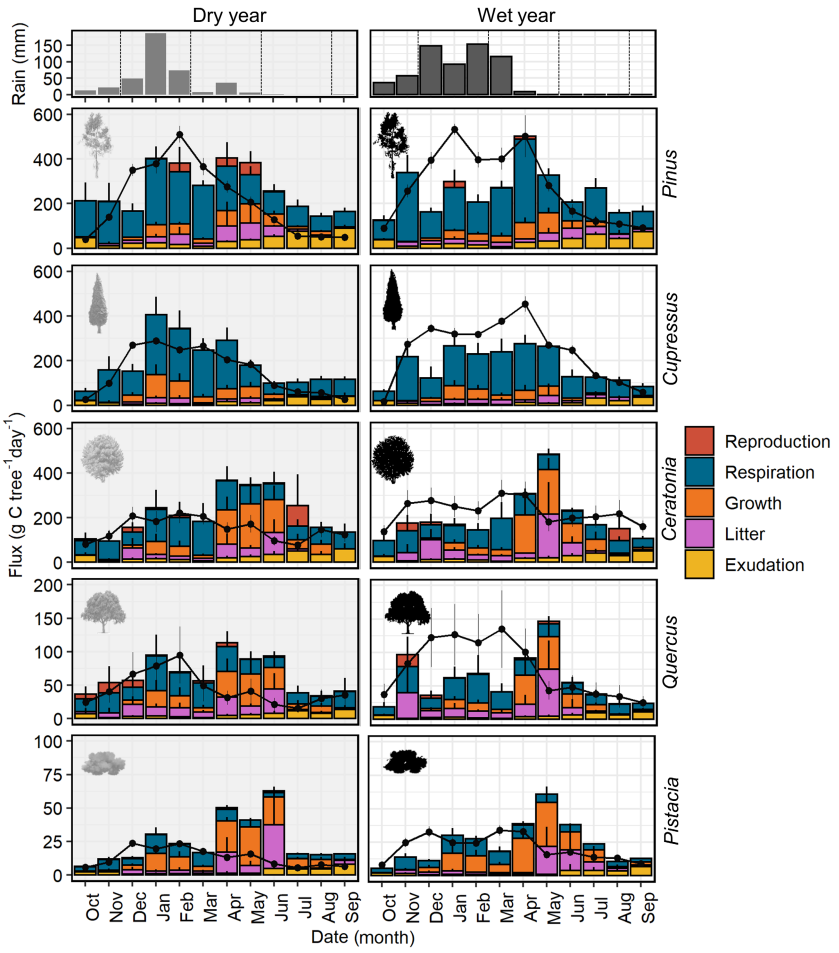

FIGURE 3 Monthly flux dynamics in dry and wet years in five species of the mixed Mediterranean forest. Assimilation is presented in line, while the five main carbon sinks are presented in stack bars: reproduction, respiration, growth, litter, and exudation ($n=4$, SE among the four individuals, and several measurements in the same month). The upper panel is the monthly precipitation amount taken from the Beit Jimal meteorological station located 1 km from the forest plot (vertical lines dividing between seasons).

(*year*×*species*, $F_{4,39}=2.448$, $p>.048$, except *Cupressus* winter–autumn). The highest amount of soluble sugars was detected in *Pistacia* (>5%), *Ceratonia* (3–4%), and a similar percentage (ca. 2%) in the three other species. High starch values were detected in *Cupressus* in autumn, *Quercus* in winter, and soluble sugars in *Ceratonia* in autumn and winter in the wet year. While, significantly, low-soluble sugars were detected in *Pistacia* at spring in the wet year. Among the soluble sugars, fructose was dominant in *Cupressus* and *Quercus*, while sucrose was dominant in *Pistacia* (Figure S7). In addition, lipid concentrations were relatively higher in *Pinus*, *Ceratonia*, and *Pistacia* related to *Cupressus* and *Quercus* (Figure S8).

3.4 | Seasonal dynamics of $\delta^{13}C$

In the measured branches, we found significant differences in $\delta^{13}C$ among species in the dry over the wet year (*species*×*year*; $F_{4,39}=2.42$, $p=.047$), inferring differences in water stress. In addition, we found ^{13}C enrichment in the dry seasons (summer and autumn) in *Ceratonia* and *Pistacia* that indicates lower stomatal conductance (*species*×*year*×*season*; $F_{12,39}=1.77$, $p=.055$, Table S8). Overall, mean values of branch $\delta^{13}C$ were ca. 1.5‰ higher in conifers than broadleaves (Figure S9). Among the two conifers, *Cupressus* $\delta^{13}C$ values were less negative, −24.6 ± 0.8, while *Pinus* were − 25.3 ± 0.8. In broadleaves, *Quercus* values were −26.7 ± 0.7, *Pistacia* − 26.9 ± 0.6, and *Ceratonia* with the wide value range of −28.5 ± 0.8.

3.5 | Forest-scale tree C allocation

Integrating our species-level assessments to the forest level (transforming from C tree^{-1} day^{-1} to C m^{-2} year^{-1}), more C is allocated belowground during the dry year. We estimate the forest canopy net assimilation at 1368.6 ± 86.2 and 2139.8 ± 118 (g C m^{-2} year^{-1}) in the dry and wet years, respectively (Figure 6). Aboveground respiration sink was significantly lower in the dry year (417.7 vs. 625.6 g C m^{-2} year^{-1}), accounting for 22.7% and 36.3% of the total tree C sinks, respectively (*year*×*flux*×*above/below*; $F_{2,17}=7.82$, $p=.001$; Table S9). However, belowground respiration sink was higher in the dry year (642.1 g C m^{-2} year^{-1}) compared to the wet year (404.8 g C m^{-2} year^{-1}), accounting for 34.9% and 23.5% of the total tree C sinks, respectively.

4 | DISCUSSION

Comparing C allocation in dry and wet years in an evergreen mixed forest, we found that in the dry year, C uptake was lower, C use was

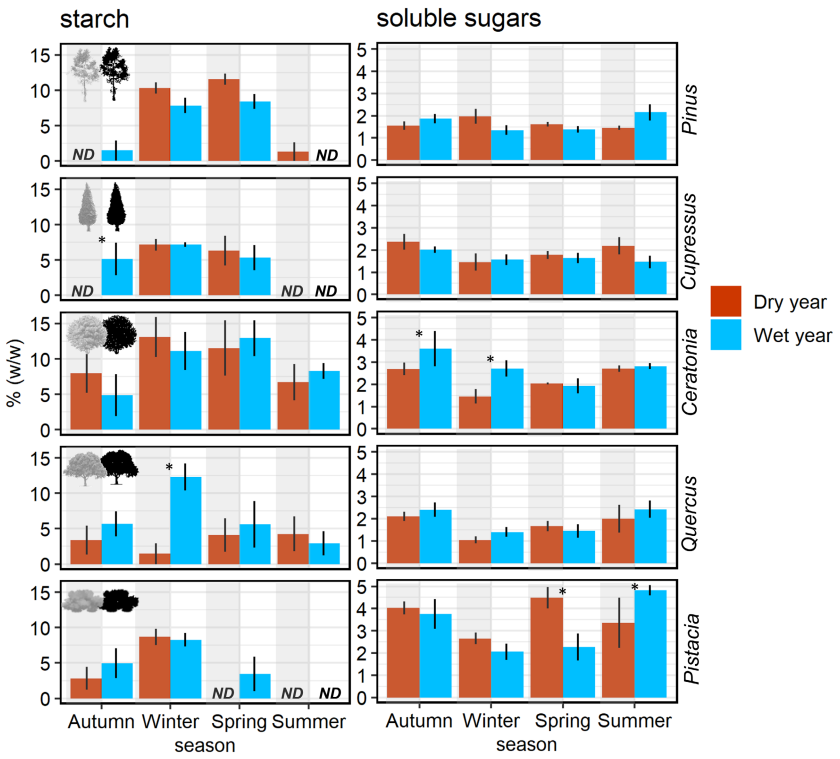

FIGURE 4 Nonstructural carbohydrate (NSC) percentage in the different seasons and years in five species of the mixed Mediterranean forest. NSC measured compounds, divided into starch and soluble sugars (sucrose, fructose, and glucose), in seasonal dynamics in the dry year (2018) and wet year (2019). Significant differences among seasons are presented in asterisks, $n = 4$.

unchanged, and C allocation to belowground sinks and reproduction was higher. This enhancement of belowground C fluxes and reproduction was found in other water-limited plants (Brunn et al., 2022; Hesse et al., 2021), although never in the context of the full tree C balance, which was done here for the first time. Assuming water is the main limiting factor in the Mediterranean region, the greater belowground allocation of C in the dry years and seasons might improve water and nutrient uptake (first hypothesis). Following our second hypothesis, low precipitation in the dry year reduced assimilation (Figures 1 and 6). However, no significant parallel reduction in C sinks was observed. According to the aboveground NSC quantity and growth amounts, there was no significant reduction in the dry versus the wet year (Figure 4), contrary to our third hypothesis. Altogether, our detailed tree-level C allocation revealed high variability among species, specifically between conifers and broadleaves. This research improves the understanding of forest strategies in drought years and promotes tree-level C allocation research, specifically belowground fluxes.

4.1 | C partitioning among tree fluxes and compartments

The studied mixed forest combines trees from different species and functional groups, each managing its C balance using different C allocation strategies. Respiration was the main C flux in this mixed forest (58.7%), respired mainly by the larger conifers *Pinus* and *Cupressus* (Figure 2). The other C sinks in the C balance here were growth (18.6%), exudation (9.7%), litter (11.4%), and reproduction (1.6%). This partitioning is similar to previous estimates for other forest types (Grayston et al., 1997; Klein & Hoch, 2015; Nygren et al., 1996), although those studies considered partitioning to three or fewer sinks while we considered five sinks (Figure 2). Compared with most forest types, our calculations were within the same range (respiration 43–73%, growth 5–27%, litter 13–34%; Klein & Hoch, 2015). The Mediterranean C allocation patterns reported here were comparable to the C partitioning of a warm Mediterranean evergreen forest (Luyssaert et al., 2007), where partitioning ratios were 43, 27, and 30% for respiration, growth, litter, and exudation, respectively. However, related to the growth fraction, the forest studied here was more similar to the extensively studied semi-arid forest in Yatir, Israel (e.g., respiration 70%, growth 17%, and litter and exudation 13%). The low partitioning to growth and litter in the forest studied here can be explained by the fact that broadleaf species are evergreen compared to many of broadleaf forests in more temperate climates, which are predominantly deciduous.

4.2 | Conifers grow fast with risk while broadleaf grow slow and safe

Different species of trees adopted a variety of C-allocation strategies to cope with the diverse environmental conditions. In this study, we measured tree C allocation in five tree species with diverse physiological and ecological characteristics belonging to different phylogenetic groups (i.e., conifers and broadleaves). The five studied species are shade tolerant (*Quercus*, *Ceratonia*, and *Pistacia*) versus intolerant (*Pinus*, *Cupressus*; Valladares & Niinemets, 2008). The two conifers, which are also tree species with light-demanding characteristics, allocated more C to respiration flux, invested less in C storage, and remained with almost no aboveground NSC at the end of

the dry season (Figure 2, Figure 4). In the same pine species, 50 km south, growth arrest and a decrease in stem diameter were shown as the first "early warning" indicators for tree mortality (Preisler et al., 2021). In comparison, the understory tree species that are shade tolerant had low respiration flux, high leaf growth, and high NSC levels (except the *Pistacia*). We detected a significant reduction in soluble sugars in the branches of *Pistacia* and in the starch of *Ceratonia* in the dry year, but not in the other tree species. In agreement, higher $\delta^{13}C$ values were detected in *Ceratonia* and *Pistacia* and compared to the other tree species (Figure 5), which suggests a reduction in stomatal conductance. Interestingly, *Quercus* presents an opposite phenomenon of high starch values in the wet year and significantly higher $\delta^{13}C$ values, possibly because of the high amounts of starch that is relatively ^{13}C enriched (Bowling et al., 2008) and the stringency of stomatal regulation (Alon et al., 2023).

Among the broadleaves, other physiological mechanisms like root depth seem to be more prominent. *Ceratonia* was photosynthetically active during nearly the entire year (Figure 3), probably because of access to deep soil water (Rog, Tague, et al., 2021) and less competition on water supply with the other shallow-rooted tree species in the dry seasons. In contrast, *Pistacia* trees are based mainly on shallow roots and compete with other species for the same water layer. Accordingly, *Pistacia* may not be able to increase photosynthesis in the wet year and was affected by the reduced water availability in the dry year. It can be speculated that the high-risk strategy used by the planted conifers in this semi-constructed forest will lead to their mortality following consecutive years of drought, as previously described in a mono-species pine forest in a semi-arid forest (Preisler et al., 2021). This decline of the conifers may lead to encroachment by the more "conservative" broad-leaved species, which assimilate less carbon, corresponding with global trends of vegetation decline with increasing aridity (Berdugo et al., 2022).

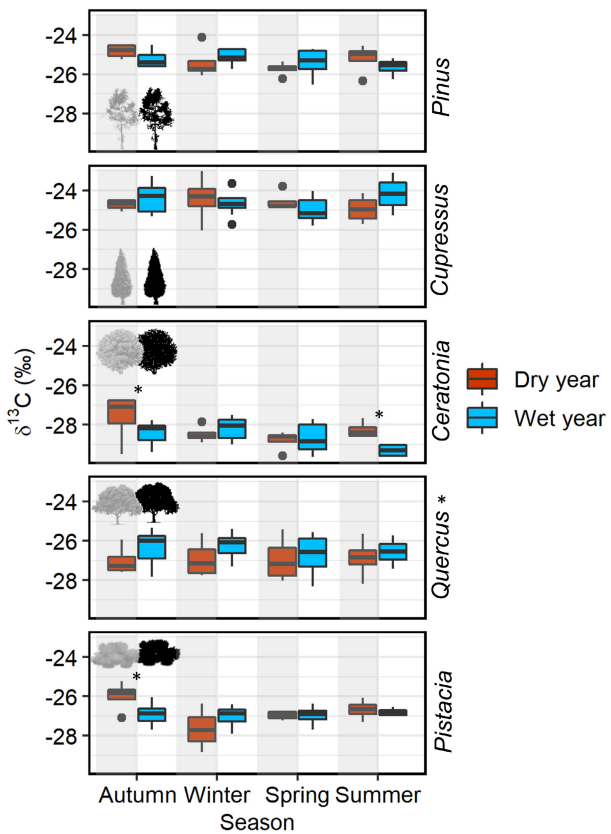

FIGURE 5 Seasonal bulk-stem $\delta^{13}C$ in five species of the mixed Mediterranean forest collected in dry (2018) and wet (2019) years. Significant differences among seasons are presented in asterisks, $n = 4–10$.

4.3 | Precipitation as the main environmental factor of tree carbon allocation in the Mediterranean region

Trees from the same species can function differently in different environmental conditions (Alon et al., 2023). For example, *Pinus halepensis* shows regional and local activity shifts according to temperature, precipitation, and other environmental parameters (Rohatyn et al., 2018). Greater assimilation fluxes were calculated in the Mediterranean region (annual rainfall of 520 mm, 7 km north from our site) than in a semi-arid region (280 mm, 50 km south), while comparable values were observed in the humid Mediterranean forest (710 mm, 200 km north; Asaf et al., 2013). Similarly, a *Pinus* tree in the semi-arid forest assimilates 25 kg C year^{-1} (Klein & Hoch, 2015), compared to a ca. 100 kg C year^{-1} in the mixed forest (Figure 2), in accordance with their size differences (fourfold C content in the latter; Table S2). This large divergence is supported by observations using other methods such as eddy covariance and carbonyl sulfide in equivalent sites (Asaf et al., 2013; Stimler et al., 2010). The synthesis of our results with results from the humid Mediterranean forest revealed comparable assimilation flux, although precipitation amounts are 1.4 times higher in the more humid forest (Figure 6). Since, as we present here, C allocation was sensitive to precipitation amount, we can assume more C allocation variation in more heterogeneous precipitation regimes.

Drought effects on C allocation can lag for longer time periods than our 2-year study (Anderegg et al., 2015; Wagner et al., 2021). In evergreen species as studied here, adjustments in whole-tree leaf area can translate into lagged effects, for example, through changes in C source and leaf respiration. In our case, the years 2016 and 2017 were also dry (Figure 1), so the 2018 responses potentially included the cumulative effect of 3-year below-average precipitation. In addition, the sequence of dry years in this study can amplify the belowground C allocation and drought legacy response (Wu et al., 2018). Understanding the legacy drought response on the plasticity of C allocation patterns for different species requires several years of C balance measurements.

4.4 | Belowground C allocation

Mediterranean forests exhibit the highest belowground plant proportion (Ma et al., 2021). Quantifying the specific C amounts trees allocate belowground still contains large uncertainties, specifically related

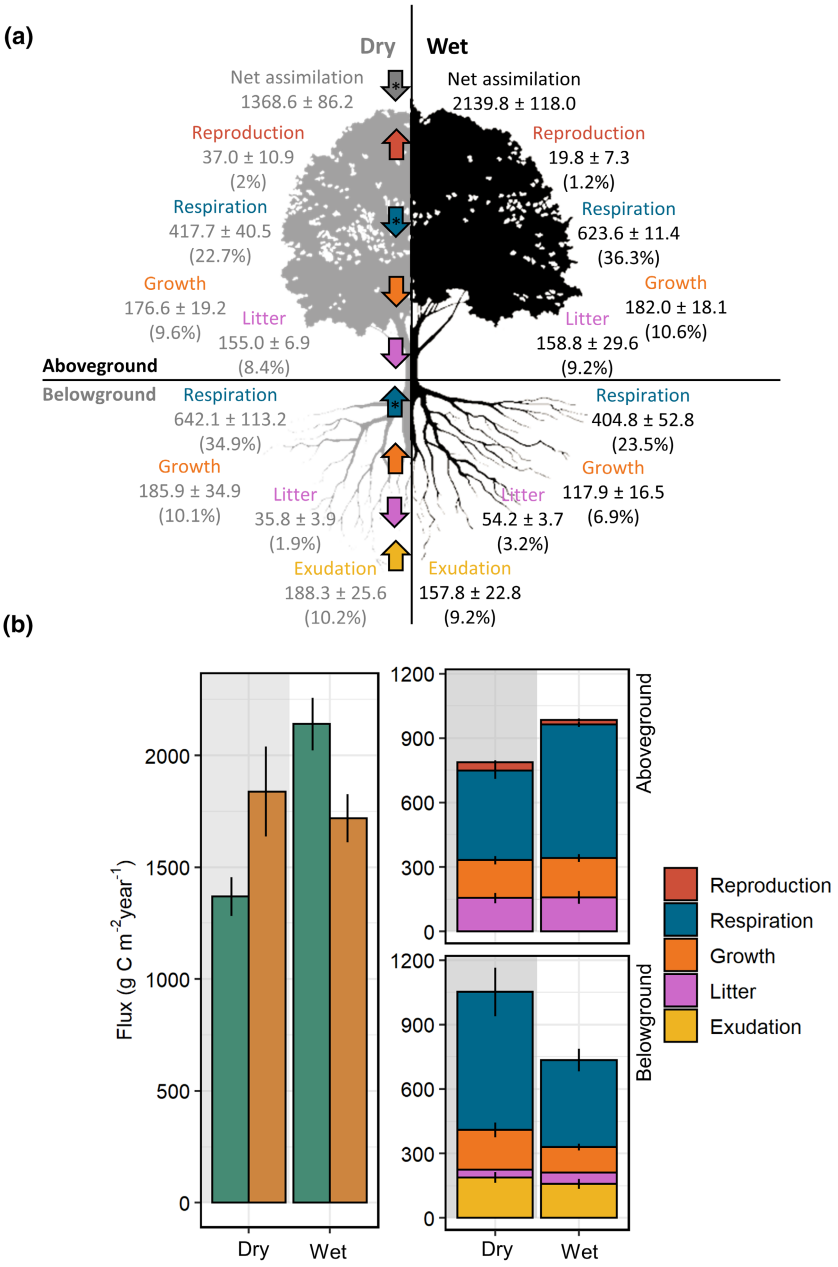

FIGURE 6 Aboveground and belowground forest tree carbon allocation dynamics in response to the dry versus wet year. (a) Forest tree carbon (C) fluxes on dry (left) and wet (right) years are divided into the aboveground (top) and belowground (bottom). Numbers show the tree C fluxes in ($g\,C\,tree^{-1}\,year^{-1}$), and the numbers in brackets are the relative percentage (%) from the entire tree C sinks. Significant differences among the years are presented in arrows; size represents the normalized effect. (b) Forest tree-level response to the dry year related to the wet year. Tree fluxes were combined for all five species and divided into aboveground and belowground. Carbon source (assimilation) and sum of the five main C sinks and carbon partitioning to the five main C sinks: reproduction, respiration, growth, litter, and exudation dividing to aboveground and belowground allocation panels. The gray background represents the dry year.

to root exudation. The estimated amount of C trees exudate to the soil ranges from 1%–5% (Brunn et al., 2022; Pinton et al., 2007) to 5%–10% (Jones et al., 2004) and can get up to 30%–40% in seedlings (Lynch, 1990). Here, the relatively high value of 9%–10% (Figures 2 and 6) is in the range of other experiments measured in this site plot and can be explained by the comparatively dry conditions in this Mediterranean forest soil. In agreement, greenhouse experiments and field experiments found higher root exudation rates under drought (Gargallo-Garriga et al., 2018; Jakoby et al., 2020). We speculate that trees in the Mediterranean region exudate more C into the soil because of the relatively dry environment and rely on the interaction with microbes for water and nutrient uptake (Bastida et al., 2017).

The Mediterranean forest is located between the arid and temperate regions, leading to considerable precipitation variation among years. Increasing C allocation belowground supports a more effective root system for uptaking water and nutrients, specifically in the Mediterranean region (Martin-StPaul et al., 2013; Misson et al., 2011; Padilla & Pugnaire, 2007). Our study compared aboveground to belowground tree C investment, reaching 50% and even larger belowground allocation in conifers (Figure 2). The conifers dominated the belowground respiration flux in the studied soil horizons (broadleaves respiration might dominate deeper soil (Rog, Tague, et al., 2021), which is outside the scope of the current research). Belowground respiration peaked twice, after the first rain event (Oct), probably reflecting the Birch effect (Jarvis et al., 2007), and again around Jan–Apr (Figure 3) and more extensively in the dry year (Figure 6). Another less known belowground flux is the root litter, estimated to constitute around 20% of NPP globally (McCormack et al., 2015). Furthermore, forest type and tree species were found to change the root decomposition rate, with the

Mediterranean forest the most prominent, and *Quercus* fine roots are faster to decompose than *Pinus* (Wambsganss et al., 2022). In agreement, the belowground C sink was found to be an important component in the global C cycle as calculated in a semi-arid forest 50 km south of this forest site (Qubaja, Grünzweig, et al., 2020; Qubaja, Tatarinov, et al., 2020). Still, more research is required to quantify the residence time of this belowground C in the mixed Mediterranean forest.

NSC annual and seasonal storage dynamics can define the resilience of each tree species to dry conditions. The aboveground NSC dynamics are well known (Hoch et al., 2003), but not much is known about belowground NSC. Our C allocation measurement measured aboveground NSC (including branches and stems) and lipid content; however, the belowground storage was lacking (Figure 4; Figures S7 and S8). Aboveground NSC influences tree resilience to drought in some (O'Brien et al., 2014; Signori-Müller et al., 2021), but not all forest types (Körner, 2003; Millard et al., 2007). In some tree species, the belowground NSC storage is the essential reservoir, accounting for >50% of the total tree NSC (Montague et al., 2022). Assuming accurate measurements of the entire aboveground and belowground C fluxes, the C deficiency in the dry year can be supplemented by the long-term belowground internal storage. Calculating the maximum NSC content for the different tree species based on our measurements and belowground values taken from the literature explains the "missing" C pool for the C balance in the dry year (Figure S10 and Table S10). In *Ceratonia* and *Quercus*, the total C pool was higher than the sum of the C sink, while in *Pinus*, *Cupressus*, and *Pistacia*, it was negligibly lower but still within the error range. We can speculate that the belowground storage stock was depleted during the three dry years preceding our study (Figure 1) and that the trees allocated large amounts of C for replenishing this storage stock in wet years. However, more research is required to understand belowground C storage and its capacity to buffer source-sink dynamics.

5 | CONCLUSIONS

We present here a unique dataset of C mass balance for five species in a mixed forest. We found that during a dry year, the total amount of C consumed was equal to wet-year consumption, but a greater C fraction was allocated belowground. While we measured at one site for 2 years, we found a novel mechanism in which the C source was more sensitive to drought than the sum of the C sinks, although specific sinks can be far more sensitive. Moreover, having measured most of the tree C fluxes directly, we bring the most detailed and reliable evidence so far to this phenomenon. Our suggested mechanism, based on tree-level carbon allocation, can help to explain other retrospective analyses based on stable isotopes, tree rings, and remote sensing (Jucker et al., 2017; Schnabel et al., 2022). A comprehensive model including the detailed C allocation mechanism and long-term existing data from other forests exposed to drought can shed light on the survival of forests in future climatic conditions.

AUTHOR CONTRIBUTIONS

Ido Rog: Data curation; formal analysis; investigation; methodology; project administration; writing – original draft; writing – review and editing. **Boaz Hilman:** Data curation; formal analysis; methodology; writing – review and editing. **Hagar Fox:** Data curation; formal analysis; methodology; writing – review and editing. **David Yalin:** Data curation; formal analysis; methodology; writing – review and editing. **Rafat Qubaja:** Data curation; formal analysis; methodology; writing – review and editing. **Tamir Klein:** Conceptualization; formal analysis; funding acquisition; investigation; methodology; project administration; resources; supervision; writing – review and editing.

ACKNOWLEDGMENTS

Shacham Megidish and Assaf Jakoby are acknowledged for the field measurements assistance. Roy More is acknowledged for the Minirhizotron measurements. The study was facilitated by multiple students and helpers within the WIS Tree Lab (Mor Lerner, Akbar Akhmedov, and Gilad Jakoby). Special thanks to Moshe Goldsmith for the NSC analysis. We thank Christin Leschik and Anett Enke from the Max Planck Institute for Biogeochemistry for lipid and NSC analysis. Stav Livne-Luzon and Efrat Dener are acknowledged for the GLM statistical design. The authors would like to thank the Jewish National Fund (KKL) for supporting the research at the Yishi forest research plot. Prof. Dan Yakir and his group (WIS) are acknowledged for providing the mobile laboratory and soil respiration measurement equipment. The project was funded in part by the European Research Council project RHIZOCARBON, granted to TK. IR is supported by the Sustainability and Energy Research Initiative Ph.D. Fellowship.

CONFLICT OF INTEREST STATEMENT

The authors declare no competing interests in the preparation of this paper.

DATA AVAILABILITY STATEMENT

The data that support the findings of this study are openly available in Zenodo at https://doi.org/10.5281/zenodo.10512572, reference number 10512572.

ORCID

Ido Rog https://orcid.org/0000-0002-9120-3617
Boaz Hilman https://orcid.org/0000-0003-3403-1561
Hagar Fox https://orcid.org/0000-0001-6905-4187
David Yalin https://orcid.org/0000-0002-0248-4913
Rafat Qubaja https://orcid.org/0000-0001-6719-9606
Tamir Klein https://orcid.org/0000-0002-3882-8845

REFERENCES

Ågren, G., Axelsson, B., Flower-Ellis, J., Linder, S., Persson, H., Staaf, H., & Troeng, E. (1980). Annual carbon budget for a young Scots pine. *Ecological Bulletins*, *32*, 307–313.

Alon, A., Cohen, S., Burlett, R., Hochberg, U., Lukyanov, V., Rog, I., Klein, T., Cochard, H., Delzon, S., & David-Schwartz, R. (2023). Acclimation

limits for embolism resistance and osmotic adjustment accompany the geographical dry edge of Mediterranean species. *Functional Ecology*, *37*, 1421–1435.

Anderegg, W. R., Schwalm, C., Biondi, F., Camarero, J. J., Koch, G., Litvak, M., Ogle, K., Shaw, J. D., Shevliakova, E., & Williams, A. (2015). Pervasive drought legacies in forest ecosystems and their implications for carbon cycle models. *Science*, *349*, 528–532.

Asaf, D., Rotenberg, E., Tatarinov, F., Dicken, U., Montzka, S. A., & Yakir, D. (2013). Ecosystem photosynthesis inferred from measurements of carbonyl sulphide flux. *Nature Geoscience*, *6*, 186–190.

Babst, F., Bouriaud, O., Papale, D., Gielen, B., Janssens, I. A., Nikinmaa, E., Ibrom, A., Wu, J., Bernhofer, C., & Köstner, B. (2014). Above-ground woody carbon sequestration measured from tree rings is coherent with net ecosystem productivity at five eddy-covariance sites. *New Phytologist*, *201*, 1289–1303.

Baldocchi, D., Falge, E., Gu, L., Olson, R., Hollinger, D., Running, S., Anthoni, P., Bernhofer, C., Davis, K., & Evans, R. (2001). FLUXNET: A new tool to study the temporal and spatial variability of ecosystem-scale carbon dioxide, water vapor, and energy flux densities. *Bulletin of the American Meteorological Society*, *82*, 2415–2434.

Bastida, F., Torres, I. F., Andrés-Abellán, M., Baldrian, P., López-Mondéjar, R., Větrovský, T., Richnow, H. H., Starke, R., Ondoño, S., & García, C. (2017). Differential sensitivity of total and active soil microbial communities to drought and forest management. *Global Change Biology*, *23*, 4185–4203.

Berdugo, M., Vidiella, B., Solé, R. V., & Maestre, F. T. (2022). Ecological mechanisms underlying aridity thresholds in global drylands. *Functional Ecology*, *36*, 4–23.

Bligh, E. G., & Dyer, W. J. (1959). A rapid method of total lipid extraction and purification. *Canadian Journal of Biochemistry and Physiology*, *37*, 911–917.

Bowling, D. R., Pataki, D. E., & Randerson, J. T. (2008). Carbon isotopes in terrestrial ecosystem pools and CO_2 fluxes. *New Phytologist*, *178*, 24–40.

Brunn, M., Hafner, B. D., Zwetsloot, M. J., Weikl, F., Pritsch, K., Hikino, K., Ruehr, N. K., Sayer, E. J., & Bauerle, T. L. (2022). Carbon allocation to root exudates is maintained in mature temperate tree species under drought. *New Phytologist*, *235*, 965–977.

Brunn, M., Krüger, J., & Lang, F. (2023). Experimental drought increased the belowground sink strength towards higher topsoil organic carbon stocks in a temperate mature forest. *Geoderma*, *431*, 116356.

Chiang, F., Mazdiyasni, O., & AghaKouchak, A. (2021). Evidence of anthropogenic impacts on global drought frequency, duration, and intensity. *Nature Communications*, *12*, 1–10.

Crowther, T. W., Van den Hoogen, J., Wan, J., Mayes, M. A., Keiser, A., Mo, L., Averill, C., & Maynard, D. S. (2019). The global soil community and its influence on biogeochemistry. *Science*, *365*, eaav0550.

Dror, D., & Klein, T. (2022). The effect of elevated CO_2 on aboveground and belowground carbon allocation and eco-physiology of four species of angiosperm and gymnosperm forest trees. *Tree Physiology*, *42*(4), 831–847.

Epron, D., Bahn, M., Derrien, D., Lattanzi, F. A., Pumpanen, J., Gessler, A., Hogberg, P., Maillard, P., Dannoura, M., Gerant, D., & Buchmann, N. (2012). Pulse-labelling trees to study carbon allocation dynamics: A review of methods, current knowledge and future prospects. *Tree Physiology*, *32*, 776–798.

Farquhar, G. D., & Busch, F. A. (2017). Changes in the chloroplastic CO_2 concentration explain much of the observed Kok effect: A model. *New Phytologist*, *214*, 570–584.

Furze, M. E., Huggett, B. A., Aubrecht, D. M., Stolz, C. D., Carbone, M. S., & Richardson, A. D. (2019). Whole-tree nonstructural carbohydrate storage and seasonal dynamics in five temperate species. *New Phytologist*, *221*, 1466–1477.

Gallucci, M. (2024). GAMLj3: GAMLj suite for linear models. R package version 3.2.0.

Gao, D., Joseph, J., Werner, R. A., Brunner, I., Zürcher, A., Hug, C., Wang, A., Zhao, C., Bai, E., & Meusburger, K. (2021). Drought alters the carbon footprint of trees in soils—Tracking the spatio-temporal fate of ^{13}C-labelled assimilates in the soil of an old-growth pine forest. *Global Change Biology*, *27*, 2491–2506.

Gargallo-Garriga, A., Preece, C., Sardans, J., Oravec, M., Urban, O., & Peñuelas, J. (2018). Root exudate metabolomes change under drought and show limited capacity for recovery. *Scientific Reports*, *8*, 1–15.

Gill, R. A., & Jackson, R. B. (2000). Global patterns of root turnover for terrestrial ecosystems. *The New Phytologist*, *147*, 13–31.

Grayston, S., Vaughan, D., & Jones, D. (1997). Rhizosphere carbon flow in trees, in comparison with annual plants: The importance of root exudation and its impact on microbial activity and nutrient availability. *Applied Soil Ecology*, *5*, 29–56.

He, W., Liu, H., Qi, Y., Liu, F., & Zhu, X. (2020). Patterns in nonstructural carbohydrate contents at the tree organ level in response to drought duration. *Global Change Biology*, *26*, 3627–3638.

Hesse, B. D., Hartmann, H., Rötzer, T., Landhäusser, S. M., Goisser, M., Weikl, F., Pritsch, K., & Grams, T. E. (2021). Mature beech and spruce trees under drought–higher C investment in reproduction at the expense of whole-tree NSC stores. *Environmental and Experimental Botany*, *191*, 104615.

Hilman, B., & Angert, A. (2016). Measuring the ratio of CO_2 efflux to O_2 influx in tree stem respiration. *Tree Physiology*, *36*, 1422–1431.

Hoch, G., & Körner, C. (2012). Global patterns of mobile carbon stores in trees at the high-elevation tree line. *Global Ecology and Biogeography*, *21*, 861–871.

Hoch, G., Richter, A., & Körner, C. (2003). Non-structural carbon compounds in temperate forest trees. *Plant, Cell & Environment*, *26*, 1067–1081.

Jakoby, G., Rog, I., Megidish, S., & Klein, T. (2020). Enhanced root exudation of mature broadleaf and conifer trees in a Mediterranean forest during the dry season. *Tree Physiology*, *40*, 1595–1605.

Jarvis, P., Rey, A., Petsikos, C., Wingate, L., Rayment, M., Pereira, J., Banza, J., David, J., Miglietta, F., Borghetti, M., Manca, G., & Valentini, R. (2007). Drying and wetting of Mediterranean soils stimulates decomposition and carbon dioxide emission: The "Birch effect". *Tree Physiology*, *27*(7), 929–940. https://doi.org/10.1093/treephys/27.7.929

Jones, D. L., Hodge, A., & Kuzyakov, Y. (2004). Plant and mycorrhizal regulation of rhizodeposition. *New Phytologist*, *163*, 459–480.

Joos, F., Prentice, I. C., Sitch, S., Meyer, R., Hooss, G., Plattner, G. K., Gerber, S., & Hasselmann, K. (2001). Global warming feedbacks on terrestrial carbon uptake under the intergovernmental panel on climate change (IPCC) emission scenarios. *Global Biogeochemical Cycles*, *15*, 891–907.

Joseph, J., Gao, D., Backes, B., Bloch, C., Brunner, I., Gleixner, G., Haeni, M., Hartmann, H., Hoch, G., & Hug, C. (2020). Rhizosphere activity in an old-growth forest reacts rapidly to changes in soil moisture and shapes whole-tree carbon allocation. *Proceedings of the National Academy of Sciences*, *117*, 24885–24892.

Jucker, T., Caspersen, J., Chave, J., Antin, C., Barbier, N., Bongers, F., Dalponte, M., van Ewijk, K. Y., Forrester, D. I., & Haeni, M. (2017). Allometric equations for integrating remote sensing imagery into forest monitoring programmes. *Global Change Biology*, *23*, 177–190.

Kattge, J., Bönisch, G., Díaz, S., Lavorel, S., Prentice, I. C., Leadley, P., Tautenhahn, S., Werner, G. D., Aakala, T., & Abedi, M. (2020). TRY plant trait database–enhanced coverage and open access. *Global Change Biology*, *26*, 119–188.

King, J. S., Albaugh, T. J., Allen, H. L., Buford, M., Strain, B. R., & Dougherty, P. (2002). Below-ground carbon input to soil is controlled by nutrient availability and fine root dynamics in loblolly pine. *New Phytologist*, *154*, 389–398.

Klein, T., Bader, M. K. F., Leuzinger, S., Mildner, M., Schleppi, P., Siegwolf, R. T., & Körner, C. (2016). Growth and carbon relations of mature Picea abies trees under 5 years of free-air CO_2 enrichment. *Journal of Ecology*, *104*, 1720–1733.

Klein, T., & Hoch, G. (2015). Tree carbon allocation dynamics determined using a carbon mass balance approach. *The New Phytologist*, *205*, 147–159.

Klein, T., Rotenberg, E., Tatarinov, F., & Yakir, D. (2016). Association between sap flow-derived and eddy covariance-derived measurements of forest canopy CO_2 uptake. *New Phytologist*, *209*, 436–446.

Klein, T., Shpringer, I., Fikler, B., Elbaz, G., Cohen, S., & Yakir, D. (2013). Relationships between stomatal regulation, water-use, and water-use efficiency of two coexisting key Mediterranean tree species. *Forest Ecology and Management*, *302*, 34–42.

Körner, C. (2003). *Alpine plant life: Functional plant ecology of high mountain ecosystems; with 47 tables*. Springer Science & Business Media.

Landhäusser, S. M., Chow, P. S., Dickman, L. T., Furze, M. E., Kuhlman, I., Schmid, S., Wiesenbauer, J., Wild, B., Gleixner, G., & Hartmann, H. (2018). Standardized protocols and procedures can precisely and accurately quantify non-structural carbohydrates. *Tree Physiology*, *38*, 1764–1778.

Lapidot, O., Ignat, T., Rud, R., Rog, I., Alchanatis, V., & Klein, T. (2019). Use of thermal imaging to detect evaporative cooling in coniferous and broadleaved tree species of the Mediterranean maquis. *Agricultural and Forest Meteorology*, *271*, 285–294.

Le Quéré, C., Andrew, R. M., Canadell, J. G., Sitch, S., Korsbakken, J. I., Peters, G. P., Manning, A. C., Boden, T. A., Tans, P. P., & Houghton, R. A. (2016). Global carbon budget 2016. *Earth System Science Data*, *8*, 605–649.

Le Roux, X., Lacointe, A., Escobar-Gutiérrez, A., & Le Dizès, S. (2001). Carbon-based models of individual tree growth: A critical appraisal. *Annals of Forest Science*, *58*, 469–506.

Luyssaert, S., Inglima, I., Jung, M., Richardson, A. D., Reichstein, M., Papale, D., Piao, S., Schulze, E. D., Wingate, L., & Matteucci, G. (2007). CO_2 balance of boreal, temperate, and tropical forests derived from a global database. *Global Change Biology*, *13*, 2509–2537.

Lynch, J. M., & Whipps, J. M. (1990). Substrate flow in the rhizosphere. *Plant and Soil*, *129*, 1–10. https://doi.org/10.1007/BF00011685

Ma, H., Mo, L., Crowther, T. W., Maynard, D. S., van den Hoogen, J., Stocker, B. D., Terrer, C., & Zohner, C. M. (2021). The global distribution and environmental drivers of aboveground versus belowground plant biomass. *Nature Ecology & Evolution*, *5*, 1110–1122.

Marshall, J. D., Tarvainen, L., Zhao, P., Lim, H., Wallin, G., Näsholm, T., Lundmark, T., Linder, S., & Peichl, M. (2023). Components explain, but do eddy fluxes constrain? Carbon budget of a nitrogen-fertilized boreal Scots pine forest. *New Phytologist*, *239*, 2166–2179.

Martin-StPaul, N. K., Limousin, J. M., Vogt-Schilb, H., Rodríguez-Calcerrada, J., Rambal, S., Longepierre, D., & Misson, L. (2013). The temporal response to drought in a Mediterranean evergreen tree: Comparing a regional precipitation gradient and a throughfall exclusion experiment. *Global Change Biology*, *19*, 2413–2426.

McCormack, M. L., Dickie, I. A., Eissenstat, D. M., Fahey, T. J., Fernandez, C. W., Guo, D., Helmisaari, H. S., Hobbie, E. A., Iversen, C. M., Jackson, R. B., Leppalammi-Kujansuu, J., Norby, R. J., Phillips, R. P., Pregitzer, K. S., Pritchard, S. G., Rewald, B., & Zadworny, M. (2015). Redefining fine roots improves understanding of below-ground contributions to terrestrial biosphere processes. *The New Phytologist*, *207*, 505–518.

Millard, P., Sommerkorn, M., & Grelet, G.-A. (2007). Environmental change and carbon limitation in trees: A biochemical, ecophysiological and ecosystem appraisal. *New Phytologist*, *175*, 11–28.

Misson, L., Degueldre, D., Collin, C., Rodriguez, R., Rocheteau, A., Ourcival, J. M., & Rambal, S. (2011). Phenological responses to extreme droughts in a Mediterranean forest. *Global Change Biology*, *17*, 1036–1048.

Montague, M. S., Landhäusser, S. M., McNickle, G. G., & Jacobs, D. F. (2022). Preferential allocation of carbohydrate reserves belowground supports disturbance-based management of American chestnut (Castanea dentata). *Forest Ecology and Management*, *509*, 120078.

Mund, M., Kutsch, W. L., Wirth, C., Kahl, T., Knohl, A., Skomarkova, M. V., & Schulze, E.-D. (2010). The influence of climate and fructification on the inter-annual variability of stem growth and net primary productivity in an old-growth, mixed beech forest. *Tree Physiology*, *30*, 689–704.

Nygren, P., Kiema, P., & Rebottaro, S. (1996). Canopy development, CO_2 exchange and carbon balance of a modeled agroforestry tree. *Tree Physiology*, *16*, 733–745.

O'Brien, M. J., Leuzinger, S., Philipson, C. D., Tay, J., & Hector, A. (2014). Drought survival of tropical tree seedlings enhanced by non-structural carbohydrate levels. *Nature Climate Change*, *4*, 710–714.

Padilla, F., & Pugnaire, F. (2007). Rooting depth and soil moisture control Mediterranean woody seedling survival during drought. *Functional Ecology*, *21*, 489–495.

Pinton, R., Varanini, Z., & Nannipieri, P. (2007). *The rhizosphere: Biochemistry and organic substances at the soil-plant interface*. CRC press.

Poorter, L., & Kitajima, K. (2007). Carbohydrate storage and light requirements of tropical moist and dry forest tree species. *Ecology*, *88*, 1000–1011.

Preisler, Y., Tatarinov, F., Grünzweig, J. M., & Yakir, D. (2021). Seeking the "point of no return" in the sequence of events leading to mortality of mature trees. *Plant, Cell & Environment*, *44*, 1315–1328.

Qubaja, R., Grünzweig, J. M., Rotenberg, E., & Yakir, D. (2020). Evidence for large carbon sink and long residence time in semiarid forests based on 15 year flux and inventory records. *Global Change Biology*, *26*, 1626–1637.

Qubaja, R., Tatarinov, F., Rotenberg, E., & Yakir, D. (2020). Partitioning of canopy and soil CO_2 fluxes in a pine forest at the dry timberline across a 13-year observation period. *Biogeosciences*, *17*, 699–714.

Richardson, A. D. (2019). Tracking seasonal rhythms of plants in diverse ecosystems with digital camera imagery. *New Phytologist*, *222*, 1742–1750.

Rog, I., Jakoby, G., & Klein, T. (2021). Carbon allocation dynamics in conifers and broadleaved tree species revealed by pulse labeling and mass balance. *Forest Ecology and Management*, *493*, 119258.

Rog, I., Tague, C., Jakoby, G., Megidish, S., Yaakobi, A., Wagner, Y., & Klein, T. (2021). Interspecific soil water partitioning as a driver of increased productivity in a diverse mixed Mediterranean forest. *Journal of Geophysical Research: Biogeosciences*, *126*, e2021JG006382.

Rohatyn, S., Rotenberg, E., Ramati, E., Tatarinov, F., Tas, E., & Yakir, D. (2018). Differential impacts of land use and precipitation on "ecosystem water yield". *Water Resources Research*, *54*, 5457–5470.

Rueden, C. T., Schindelin, J., Hiner, M. C., DeZonia, B. E., Walter, A. E., Arena, E. T., & Eliceiri, K. W. (2017). ImageJ2: ImageJ for the next generation of scientific image data. *BMC Bioinformatics*, *18*, 529.

Ruehr, N. K., Offermann, C. A., Gessler, A., Winkler, J. B., Ferrio, J. P., Buchmann, N., & Barnard, R. L. (2009). Drought effects on allocation of recent carbon: From beech leaves to soil CO_2 efflux. *New Phytologist*, *184*, 950–961.

Sala, A., Woodruff, D. R., & Meinzer, F. C. (2012). Carbon dynamics in trees: Feast or famine? *Tree Physiology*, *32*, 764–775.

Schiestl-Aalto, P., Ryhti, K., Mäkelä, A., Peltoniemi, M., Bäck, J., & Kulmala, L. (2019). Analysis of the NSC storage dynamics in tree organs reveals the allocation to belowground symbionts in the framework of whole tree carbon balance. *Frontiers in Forests and Global Change*, *2*, 17.

Schnabel, F., Liu, X., Kunz, M., Barry, K. E., Bongers, F. J., Bruelheide, H., Fichtner, A., Härdtle, W., Li, S., & Pfaff, C.-T. (2021). Species richness stabilizes productivity via asynchrony and drought-tolerance diversity in a large-scale tree biodiversity experiment. *Science Advances*, *7*, eabk1643.

Schnabel, F., Purrucker, S., Schmitt, L., Engelmann, R. A., Kahl, A., Richter, R., Seele-Dilbat, C., Skiadaresis, G., & Wirth, C. (2022). Cumulative growth and stress responses to the 2018–2019 drought in a European floodplain forest. *Global Change Biology*, *28*, 1870–1883.

Signori-Müller, C., Oliveira, R. S., Barros, F. D. V., Tavares, J. V., Gilpin, M., Diniz, F. C., Zevallos, M. J. M., Yupayccana, C. A. S., Acosta, M., &

Bacca, J. (2021). Non-structural carbohydrates mediate seasonal water stress across Amazon forests. *Nature Communications*, *12*, 1–9.
Smith, M. G., Miller, R. E., Arndt, S. K., Kasel, S., & Bennett, L. T. (2018). Whole-tree distribution and temporal variation of non-structural carbohydrates in broadleaf evergreen trees. *Tree Physiology*, *38*, 570–581.
Stimler, K., Montzka, S. A., Berry, J. A., Rudich, Y., & Yakir, D. (2010). Relationships between carbonyl sulfide (COS) and CO_2 during leaf gas exchange. *New Phytologist*, *186*, 869–878.
Tcherkez, G., Mahé, A., Gauthier, P., Mauve, C., Gout, E., Bligny, R., Cornic, G., & Hodges, M. (2009). In folio respiratory fluxomics revealed by ^{13}C isotopic labeling and H/D isotope effects highlight the noncyclic nature of the tricarboxylic acid "cycle" in illuminated leaves. *Plant Physiology*, *151*, 620–630.
Team, R. C. (2000). *R language definition*. Vienna, Austria: R foundation for statistical computing.
Team, R. C. (2018). *R: A language and environment for statistical computing*. Vienna, Austria: R Foundation for Statistical Computing.
Tsamir-Rimon, M., Ben-Dor, S., Feldmesser, E., Oppenhimer-Shaanan, Y., David-Schwartz, R., Samach, A., & Klein, T. (2021). Rapid starch degradation in the wood of olive trees under heat and drought is permitted by three stress-specific beta amylases. *New Phytologist*, *229*, 1398–1414.
Tumber-Dávila, S. J., Schenk, H. J., Du, E., & Jackson, R. B. (2022). Plant sizes and shapes above-and belowground and their interactions with climate. *New Phytologist*, *235*, 1032–1056.
Valladares, F., & Niinemets, Ü. (2008). Shade tolerance, a key plant feature of complex nature and consequences. *Annual Review of Ecology, Evolution, and Systematics*, *39*, 237–257.
Verkouteren, R. (2006). New guidelines for $\delta^{13}C$ measurements. *Analytical Chemistry*, *78*, 2439–2441.
Wagner, Y., Pozner, E., Bar-On, P., Ramon, U., Raveh, E., Neuhaus, E., Cohen, S., Grünzweig, J., & Klein, T. (2021). Rapid stomatal response in lemon saves trees and their fruit yields under summer desiccation, but fails under recurring droughts. *Agricultural and Forest Meteorology*, *307*, 108487.
Wambsganss, J., Freschet, G. T., Beyer, F., Bauhus, J., & Scherer-Lorenzen, M. (2022). Tree diversity, initial litter quality, and site conditions drive early-stage fine-root decomposition in European forests. *Ecosystems*, *25*, 1493–1509. https://doi.org/10.1007/s10021-021-00728-3
Wegener, F., Beyschlag, W., & Werner, C. (2015). High intraspecific ability to adjust both carbon uptake and allocation under light and nutrient reduction in Halimium halimifolium L. *Frontiers in Plant Science*, *6*, 609.
Werner, C., Meredith, L. K., Ladd, S. N., Ingrisch, J., Kübert, A., van Haren, J., Bahn, M., Bamberger, I., Beyer, M., & Blomdahl, D. (2021). Ecosystem fluxes during drought and recovery in an experimental forest. *Science*, *374*, 1514–1518.
Wu, X., Liu, H., Li, X., Ciais, P., Babst, F., Guo, W., Zhang, C., Magliulo, V., Pavelka, M., & Liu, S. (2018). Differentiating drought legacy effects on vegetation growth over the temperate Northern Hemisphere. *Global Change Biology*, *24*, 504–516.
Zweifel, R., Sterck, F., Braun, S., Buchmann, N., Eugster, W., Gessler, A., Häni, M., Peters, R. L., Walthert, L., & Wilhelm, M. (2021). Why trees grow at night. *New Phytologist*, *231*, 2174–2185.
Zwetsloot, M. J., & Bauerle, T. L. (2021). Repetitive seasonal drought causes substantial species-specific shifts in fine-root longevity and spatio-temporal production patterns in mature temperate forest trees. *New Phytologist*, *231*, 974–986.

SUPPORTING INFORMATION

Additional supporting information can be found online in the Supporting Information section at the end of this article.

How to cite this article: Rog, I., Hilman, B., Fox, H., Yalin, D., Qubaja, R., & Klein, T. (2024). Increased belowground tree carbon allocation in a mature mixed forest in a dry versus a wet year. *Global Change Biology*, *30*, e17172. https://doi.org/10.1111/gcb.17172